

A glass microfluidic chip for continuous blood cell sorting by a magnetic gradient without labeling

Bai-Yan Qu · Zhi-Yong Wu · Fang Fang ·
Zhi-Ming Bai · Dong-Zhi Yang · Shu-Kun Xu

Received: 11 May 2008 / Revised: 28 August 2008 / Accepted: 1 September 2008 / Published online: 20 September 2008
© Springer-Verlag 2008

Abstract This paper presents a microfluidic chip for highly efficient separation of red blood cells (RBCs) from whole blood on the basis of their native magnetic properties. The glass chip was fabricated by photolithography and thermal bonding. It consisted of one inlet and three outlets, and a nickel wire of 69- μm diameter was positioned in the center of a separation channel with 149- μm top width and 73- μm depth by two parallel ridges (about 10 μm high). The two ridges were formed simultaneously during the wet etching of the channels. The nickel wire for generating the magnetic gradient inside the separation channel was introduced from the side of the chip through a guide channel. The external magnetic field was applied by a permanent magnet of 0.3 T placed by the side of the chip and parallel to the main separation channel. The RBCs were separated continuously from the 1:40 (v/v) diluted blood sample at a flow rate in the range 0.12–0.92 $\mu\text{L}/\text{min}$ (9–74 mm/min) with the chip, and up to 93.7% of the RBCs were collected in the middle outlet under a flow rate of 0.23 $\mu\text{L}/\text{min}$. The cell sedimentation was alleviated by adjusting the specific density of the supporting media with bovine serum albumin. Quantum dot labeling was introduced for visual fluorescence tracking of the separation process. The uneven distribution phenomenon of the blood cells around the nickel wire was reported and discussed.

Keywords Microfluidic chip · Magnetic gradient · Blood sample · Red blood cells · Quantum dot labeling

Introduction

Blood component transfusion is important in the therapy of various diseases, such as anemia, cancer, and immune disease. The principal methods for blood cell component separation for therapeutic purposes are conventional mechanical filtration using fiber and mesh, centrifugation, and magnetic separation. The centrifugation method, which has been well developed, is most widely used for various cell separations, but cell damage and aggregation could arise [1]. Magnetic gradient separation was introduced in the late 1960s for separation of paramagnetic and diamagnetic particles from water, soil, or air [2]. It was also used in the separation of blood cells [1–9] on the basis of their native magnetic properties. No magnetic force can be applied onto a magnetic-field-susceptible particle in a homogenous field; however, the particle can move in an inhomogeneous field in the direction of a magnetic gradient. Melville et al. [3] and Owen [4] demonstrated the separation by a column containing a stainless steel wire in a high magnetic field; 70% of red blood cells (RBCs) were retained with a magnetic field of 1.75 T, and 90% separation was achieved in a magnetic field as high as 3.3 T. The separations worked in a batch mode, i.e., the separation and collection were carried out alternately. Continuous magnetic separation of RBCs from whole blood was reported by Takayasu et al. [1, 5, 6] using a thin rectangular glass tube and a ferromagnetic nickel wire of 100- μm diameter in a magnetic field between 1.25 and 2 T. Zborowski et al. [7] measured the migration velocity of erythrocytes with cell tracking velocimetry. The cells were exposed to a magnetic field of 1.4 T with a mean magnetic gradient of 0.131 T/mm.

B.-Y. Qu · Z.-Y. Wu (✉) · F. Fang
Research Center for Analytical Sciences, Northeastern University,
110004 Shenyang, China
e-mail: zywu_2008@yahoo.com.cn

Z.-M. Bai
Physics Department, Northeastern University,
110004 Shenyang, China

D.-Z. Yang · S.-K. Xu
Chemistry Department, Northeastern University,
110004 Shenyang, China

The above-mentioned magnetic separations of cells were mainly performed in macro-scale systems of centimeter size, with which 90% separation of RBCs could be achieved with the application of a magnet field as high as 3.3 T. Scaling down of the separation system is an effective strategy for enhancing the performance, and the continuous RBC separation rate could reach up to 93.5% under a magnetic field of only 0.2 T [2]. Although the production rate is decreased by scaling down, it could be meaningful for clinical diagnostics where speed and low consumption of sample are important. With micro total analysis system technology, multiple analytical processes could be integrated in one single-chip device [10]. Biological analysis in chip format is favorable for reducing reagent and power consumption, shortening the analysis time, and the throughput could also be increased by parallel operation [2, 10]. Microfluidic chips with channels of cell size (10–100 μm) are especially suitable for cellular assay [11, 12], such as magnetic trapping and sorting [13–15], optical manipulation [16, 17], mechanical manipulation [18–20], and electrical trapping and sorting [21–23]. A magnetic field is a promising resource, which is clean, versatile, remote, and noninvasive for cell manipulation in a microfluidic chip [10]. Han and Frazier [2, 8, 9] reported a magnetic gradient microseparator, with which RBCs and white blood cells (WBCs) from whole blood were separated on the basis of their native magnetic difference. The chip fabrication involved microelectroformation of a nickel pattern through thick photoresist micromolds and wet chemical etching. In total, 93.5% of RBCs were separated continuously by three-stage cascade paramagnetic capture mode at a flow rate of 0.08 $\mu\text{L}/\text{min}$.

Visualization of the separation process is also important during system development. Fluorescence labeling with organic dyes is most widely used for cell imaging. Nano-scale quantum dots (QDs) as an inorganic fluorescence label have attracted attention owing to their significant advantages over organic fluorophores in terms of fluorescence intensity, resistance to photobleaching, and multiple colors that facilitate simultaneous imaging of multiple fluorophores [24–27]. These features make QDs ideal for concurrent monitoring of intracellular interactions in living cells and organisms over a period ranging from less than 1 s to several days [28]. Continuous magnetic sorting of QD-labeled cells could integrate fluorescence, magnet selectivity, and bioselectivity, and will find wider applications in fast clinical diagnosis.

This paper presents a simple glass microfluidic chip that could generate a magnetic gradient in the separation channel, and sorting of RBCs was successfully demonstrated on the basis of their native magnetic susceptibility. The performance of the chip was characterized by microscopic bright-field imaging and dark-field fluorescence imaging

with QD labeling, respectively. Cell sedimentation and uneven distribution in the channel were also studied and are discussed.

Materials and methods

Chemicals and materials

Bovine serum albumin (BSA) was purchased from Sigma. All other chemicals were of analytical grade. The supporting medium was pH 7.4 phosphate buffer without sodium chloride, unless otherwise mentioned. The QD was a homemade CdTe QD capped with mercaptopropionic acid. The 1.7-mm-thick glass substrate with a chromium layer and photoresist coating was from Shaoguang Microelectronics, Changsha, China.

Instruments

The sample solution was infused into the chip by a syringe pump from Bioanalytical Systems, USA. Microscopic imaging was carried out using an IBE2003 fluorescence microscope system from Optoelectronic Instrument, Chongqing, China, which was equipped with a CCD (YH-9616 Yonghui Technology Development, Shenzhen, China). The magnetic field strength of the neodymium iron boron permanent magnet was measured using a gauss/teslameter (HT 100 G, Hengtong Magnetolectricity, Shanghai, China). The JKG-2A lithography system was from Xueze Optical-Mechanical, Shanghai, China. The XMC 5400 temperature-programmable controller for thermal bonding of the glass chip was from Oriental Spark Intelligent Instruments, Fujian, China, and the oven (SX2-4-10) was from Electric Furnace Factory, Shenyang, China.

Chip design and microfabrication

Figure 1a illustrates the layout of the chip, with one inlet and three outlets. A permanent magnet sheet was placed parallel to the channel by the side of the chip, and the direction of the magnetic field was perpendicular to the chip channel. A nickel wire was introduced into the channel through a guide channel and was positioned in the middle of the microchannel following the methods introduced in [29]. The RBCs (as paramagnetic particles) were drawn closer to the nickel wire and the WBCs (diamagnetic particles) were forced away from the wire following the magnetic gradient induced around the nickel wire. The cross-sectional view of the separation channel and the separation principle are illustrated in Fig. 1b. The chip system was placed on the microscope stage for visual observation and optical imaging.

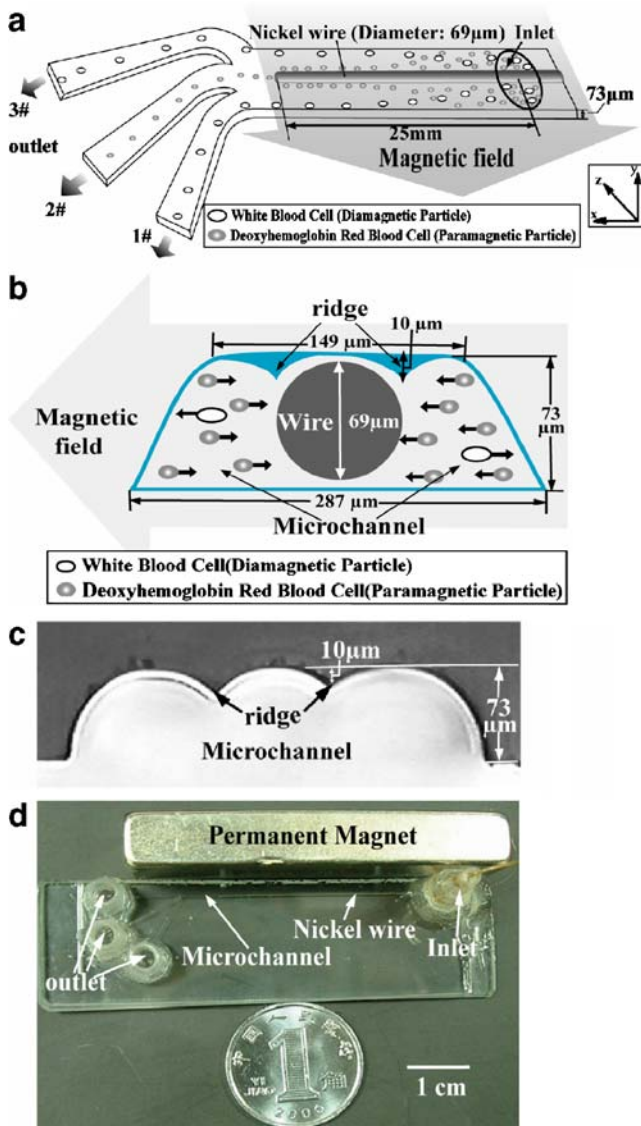


Fig. 1 The microfluidic chip with a ferromagnetic wire. **a** Perspective view of the microchannel layout that has one inlet and three outlets, with an external magnetic field applied horizontally from one side of the channel. **b** Cross section of the main channel and magnetic gradient separation of blood cells. **c** Microscopic image of the cross section of the main channel before bonding. **d** The chip system

The photolithographic process described in [30] was adopted for the fabrication of the glass chip. The ridges for aligning the nickel wire in the center of the separation channel were formed simultaneously during the etching of the main channel following a procedure developed in this laboratory [29]. The main microchannel was 73 μm in depth and the two ridges were about 10 μm in height; the microscope image is shown in Fig. 1c. The chip was thermally bonded at 580 $^{\circ}\text{C}$ in about 4 h. A nickel wire of 69- μm diameter was inserted through a guide channel into the main separation channel and positioned between the

two parallel ridges. The exit of the guide channel for inserting the nickel wire was then sealed by epoxy resin.

The side of the chip parallel to the separation channel was ground such that the distance between the channel and the side was reduced to about 2 mm. A fused-silica capillary (250- μm inner diameter) was connected to the inlet for infusion of the sample cell suspension solution by a syringe pump. The chip system is shown in Fig. 1d.

Sample preparation

The blood samples were obtained from healthy adults, and were prepared by adding 2 mg EDTA- Na_2 (as anticoagulant) to 1-mL samples [31]. The samples thus prepared were stored in a refrigerator at 4 $^{\circ}\text{C}$. The blood cell samples were prepared by 1:40 (v/v) mixing of the blood sample with 5 mM NaNO_2 solution to oxidize the hemoglobin in RBCs into paramagnetic form, and kept at 4 $^{\circ}\text{C}$ for 40 min before use following the procedure reported in [2, 4]. Some blood samples were treated in the same way, but the specific density of the supporting medium was adjusted to 1.070 by adding BSA [31].

The blood cells were labeled by CdTe QDs capped with mercaptopropionic acid, which gave green fluorescence with 488-nm excitation [32]. The QDs (0.2 mol/L) and the blood samples were 5:1 (v/v) mixed, and the mixture was maintained at 37 $^{\circ}\text{C}$ for 30 min [26, 32]. The blood samples were then washed three times and resuspended in 20 μL buffer. Then the labeled blood cells were diluted 41 times by NaNO_2 solution (specific density 1.070) and kept at 4 $^{\circ}\text{C}$ for 40 min before use.

Procedure

First, the microfluidic chip was located on the stage of microscope, and a permanent magnet was placed by one side of the microchip about 2 mm from the separation channel. The blood samples were infused into the chip constantly by the syringe pump, and the images of the separation channel were observed under the microscope by a CCD either in white light illumination or in fluorescence mode. The images were magnified 100 times and recorded by the CCD or a numerical camera. The direction of sample flow was from the right to the left in all images and the permanent magnet was located at the top in all images.

Results and discussion

Magnetic gradient microfluidic chip

In the preparation of the chip, only conventional photolithography and wet etching were involved; thus, sophisti-

cated multiple microfabrication steps were avoided for the introduction of a ferromagnetic element in the channel. The introduction of the magnetic element in the chip was simply realized by placing a single nickel (ferromagnetic) wire of 69- μm diameter into the separation channel and precisely positioned in the center of the channel after thermal bonding of the chip. A permanent magnet of 0.3 T was placed by one side of the chip and parallel to the separation channel, with one magnetic pole side facing the nickel wire in the chip channel. In this way, a magnetic gradient was effectively generated in the separation channel around the nickel wire as demonstrated in the following sections by blood cell separation without magnetic labeling.

Continuous cell separation

The native magnetic susceptibility of a RBC is due to the existence of hemoglobin in the cell. Deoxyhemoglobin contained in the RBC is paramagnetic [1, 3–7]. When the sample was treated with NaNO_2 , the hemoglobins in the RBCs turned into paramagnetic form [4]. It should be noted that the native magnetic susceptibility of RBCs is quite low compared with that of magnetically labeled cells, and they will not be separated in a uniform magnetic field [7]. In a magnetic gradient field, the force applied on a magnetic particle with weak magnetic susceptibility depends strongly on the product of the field strength and the magnetic gradient, as well as on the particle size and magnetic susceptibility, as shown by Eq. 1 [33, 34]:

$$F = \chi V H dH/dx, \quad (1)$$

where χ is the magnetic susceptibility difference between the particle and the media, V is the volume of the particle, H is the magnetic field strength, and dH/dx is the magnetic field gradient. It can be seen Eq. 1 that no magnetic force will be applied onto a magnetic-field-susceptible cell to make it move in a homogenous magnetic field (i.e., $dH/dx=0$); it is simply magnetized. With the introduction of the nickel wire in the separation channel, a magnetic gradient was induced and cell migration occurred in the direction perpendicular to the fluidic flow as demonstrated in Fig. 2a. The flow rate was 0.23 $\mu\text{L}/\text{min}$, corresponding to a velocity of about 9 mm/min in the microchannel. The applied magnetic field strength was 0.3 T as monitored by a gaussmeter. Most of the RBCs were obviously drawn toward the nickel wire in 30 min. Figure 2b shows the separation of blood cells in the outlet of the microchip. The poor smoothness of the channel edges was due to the limited resolution of the photo mask, and could be easily improved by using a high-resolution photo mask. With only one stage of separation, 93.7% of RBCs were found in the middle outlet as measured by a manual cell counter. On the other hand, no separation was observed for blood sample without NaNO_2 pretreatment

(Fig. 2c). An image similar to that in Fig. 2c was obtained with the treated sample, but without application of the magnet. Most of the cells seen in the images are RBCs, since WBCs are in the minority (1:1,000 to RBCs) and are difficult to see with a normal bright-field microscope in the separation chip owing to their transparency.

Flow rate effect

Figure 3 shows the effect of flow rate from 0.12 to 0.92 $\mu\text{L}/\text{min}$ (approximately 9–74 mm/min). It can be seen from the images that more RBCs were drawn closer to the nickel wire as the flow velocity decreased. Under a flow rate of 0.12 $\mu\text{L}/\text{min}$, more RBCs were centralized and 96%

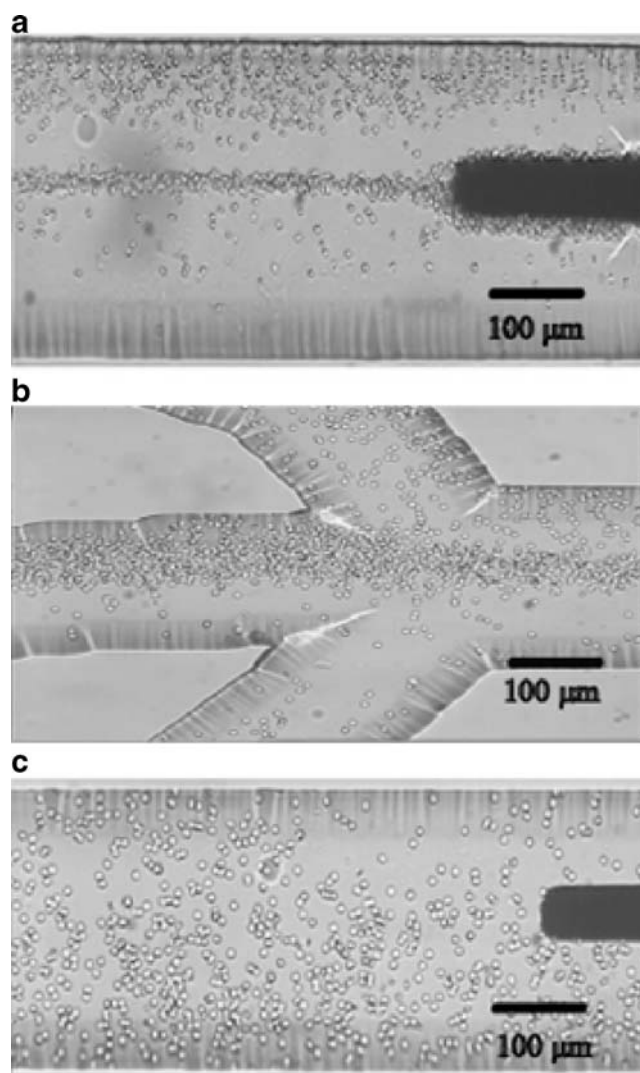


Fig. 2 Images of the blood cells passing through the microchannel, flow rate 0.23 $\mu\text{L}/\text{min}$, time 30 min, blood sample 1:40 (v/v) diluted. **a** End of the wire. **b** Outlet of the chip. **c** End of the wire, without magnetic field applied. The wire was 69 μm in diameter, and the magnet was placed at the top of the images (same as for the images in the other figures)

of RBCs were collected in the middle outlet as shown in Fig. 3a. Under flow rates of 0.23, 0.58, and 0.92 $\mu\text{L}/\text{min}$, the collection rates in the middle outlet were 93.7, 71.1, and 59.6%, respectively. The flow-rate effect could be ex-

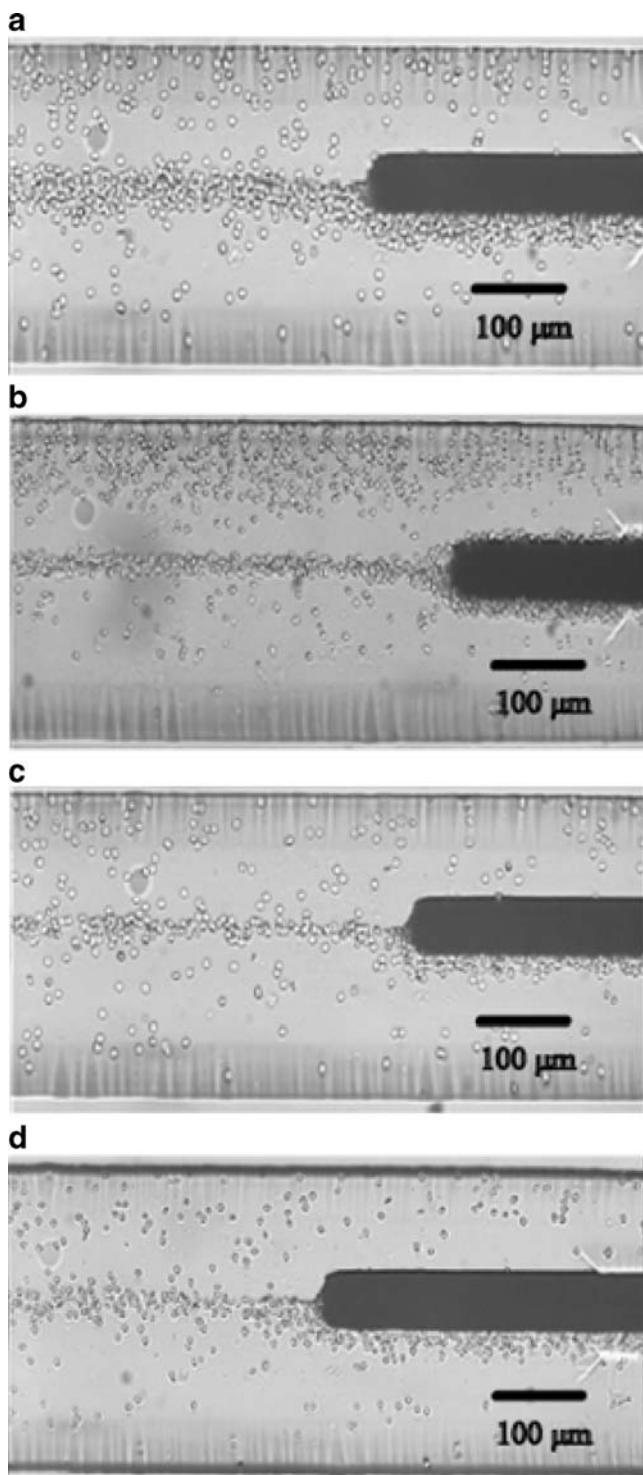


Fig. 3 Flow-rate effect. All images were taken after 30 min of sample infusion at the given flow rates. The blood sample was 1:40 (v/v) diluted. **a** 0.12 $\mu\text{L}/\text{min}$, **b** 0.23 $\mu\text{L}/\text{min}$, **c** 0.58 $\mu\text{L}/\text{min}$, **d** 0.92 $\mu\text{L}/\text{min}$

plained by the residence time: the longer the time, the more the RBCs migrate to the wire as a result of the magnetic gradient during their travel in the channel. After 30 min, fewer cells were observed under higher flow rate, since most cells were washed out of the channel by the high flow, and cell sedimentation occurred in the infusion system.

Cell sedimentation

The specific density of RBCs is 1.100 and that of WBCs is 1.060 [31]; both are greater than that of a normal aqueous medium, which is close to 1.000. Cell sedimentation is inevitable during a long assay period, though this is seldom mentioned in the related reports. Cell sedimentation could occur in the syringe, the connection tube, and the separation channel. But this had less effect on the magnetic separation, since the sedimentation and magnetic field are perpendic-

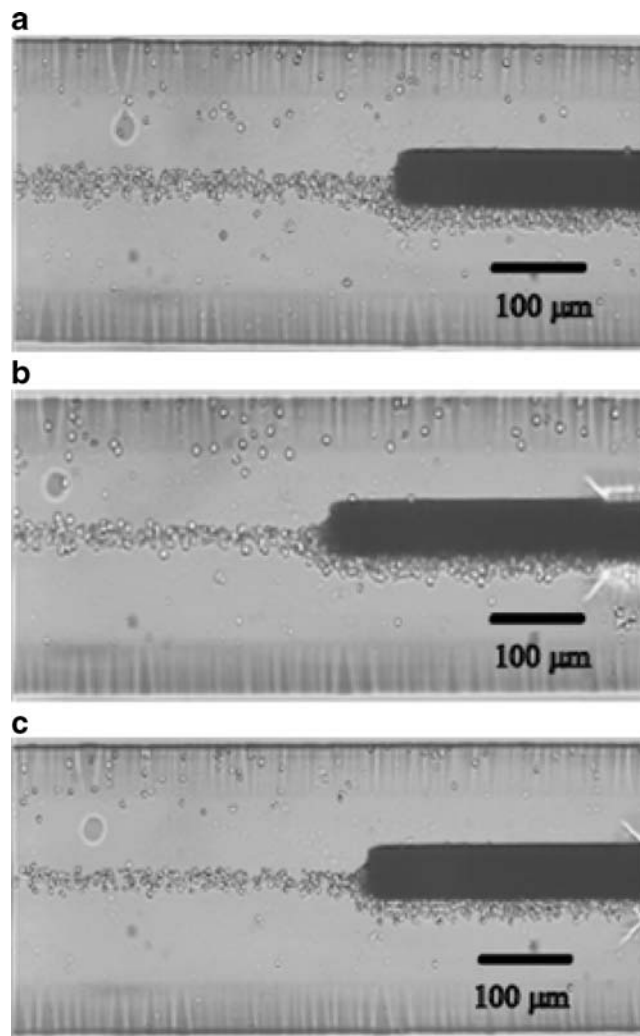


Fig. 4 Effect of specific density adjustment of supporting medium, flow rate 0.23 $\mu\text{L}/\text{min}$. The blood sample was 1:40 (v/v) diluted. **a** 30 min, **b** 60 min, **c** 90 min. The specific density of the supporting medium was adjusted to 1.070 by bovine serum albumin

ular to each other. The images observed at the end of the wire at different times up to 90 min under a given flow rate of $0.23 \mu\text{L}/\text{min}$ showed that the quantity of blood cells decreased with time (images omitted). It would be desirable to have a constant feeding of the cells into the chip in the cell separation study. To reduce the sedimentation effect, the density of the medium was adjusted by BSA, and results at 30, 60, and 90 min are shown in Fig. 4. It can be seen from the images that the sedimentation was obviously alleviated by adjusting the specific density to 1.070 with

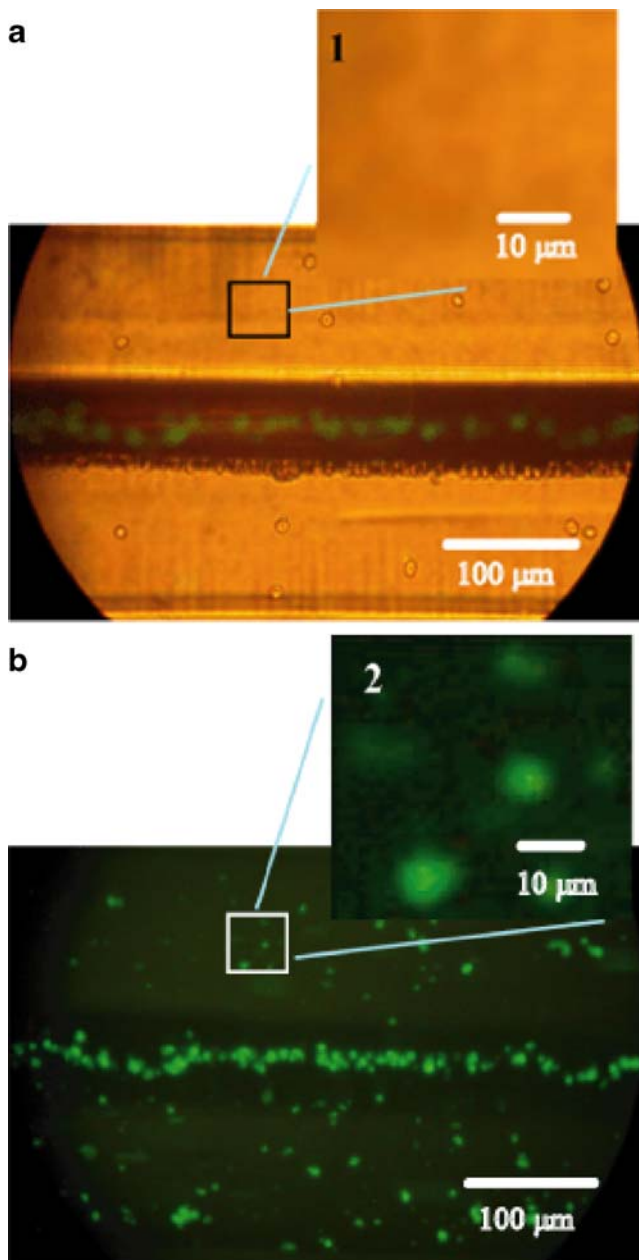


Fig. 5 Microscopic images of the blood cells labeled by quantum dots. **a** Bright-field image, with blue light on. **b** Dark-field fluorescence image. The *dark shadow* in **a** is the nickel wire of $69\text{-}\mu\text{m}$ diameter

BSA. Nevertheless, sedimentation was still noticed at 90 min as shown in Fig. 4c. More BSA resulted in a too viscous medium. Salt such as CsCl was not used because of concern of cell breakage.

QD labeling of the blood cells

QD labeling was introduced for better visualization of the magnetic separation of the cells in the chip. Since QD labeling of cells is not selective, both minority WBCs and RBCs could be seen. Figure 5 shows the images of the separation of cells labeled by QDs in the middle part of the channel under a flow rate of $0.23 \mu\text{L}/\text{min}$ for 30 min. The flow was stopped during imaging to obtain a clear image of the cells. The images in Fig. 5 were acquired under identical focusing condition, but under different illumination. The image shown in Fig. 5a was obtained with both bright light from the top of and blue excitation light from beneath the inverted microscope; thus, the cells under the wire (the dark shadow in the center) were also visible. In fluorescence mode, as shown in Fig. 5b, all types of cell in focus became clearly visible in the dark background, including WBCs away from the wire and RBCs near the wire. It is interesting to note that although WBCs are in the minority, they could still be seen in the dark field by QD labeling. It can be seen from the inserts that the fluorescence spots visible in Fig. 5b are hardly seen in Fig. 5a, and they should be attributed to the WBCs. Selective fluorescence labeling of WBCs could also be done with nucleus stain [2]. As indicated in the images in Fig. 5, the cells could travel from one side of the wire to the other. This is because the depth of the channel is about $4 \mu\text{m}$ greater than the diameter of the wire, leaving space for the cells to travel across the wire. The effective magnetic separation of QD-labeled cells also indicated that the QD labeling had no side

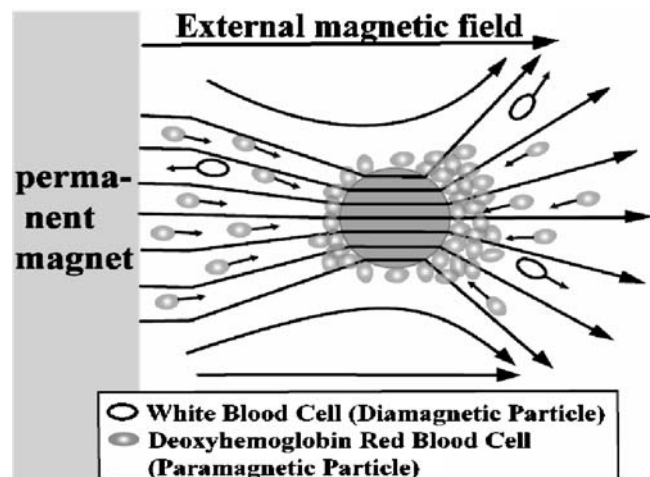


Fig. 6 The asymmetrical distribution of the blood cells around the ferromagnetic wire in the microchannel

effect on the magnetic separation. Furthermore, blue light illumination for longer than 120 min did not result in obvious fluorescence quenching, demonstrating the advantage of QD labeling for cell fluorescence visualization.

Asymmetry of the cells on the wire

It was noticed that the RBCs were attracted more to the outer side of the wire far away from the magnet, as clearly shown in Fig. 4. The magnetic sheet is longer than the separation channel, thus the edge effect should not be obvious, and the magnetic field strength along the separation channel is about the same level. However, the magnetic strength decays quickly with distance from one pole of the magnet (z direction in Fig. 1a). When an external magnetic field was applied to the ferromagnetic wire from only one side, the magnetic field was deformed near the wire, and a magnetic gradient was generated around the wire as reported in [2, 9, 33]. This is why RBCs can be attracted toward the ferromagnetic wire [2]. Since only one magnet was placed by the separation channel, the magnetic field near the nickel wire was not homogenous in the z direction. The magnetic lines disperse with distance, and resulted in a greater gradient on the outer side of the nickel wire, as indicated in Fig. 6, which gives rise to an enhanced force on the RBCs. This analytical analysis is in agreement with the experimental facts. The gap between the wire and the channel walls allowed the cells to migrate from one side of the wire to the other. Numerical simulation will be carried out in the future.

Summary

Briefly, a simplified glass microfluidic chip integrated with a magnetic gradient element was designed and prepared, with which continuous sorting of blood cells was successfully demonstrated. The magnetic gradient in the separation channel was induced by a ferromagnetic nickel wire of 69- μm diameter that was precisely positioned in the center of the main separation channel. Up to 93.7% of the RBCs were selectively collected with the chip and one 0.3-T permanent magnet. The cell sedimentation was effectively alleviated by adjusting the specific density of the supporting medium. An asymmetrical distribution of the magnetic gradient was observed experimentally with the chip by blood cell separation.

We foresee that the method proposed in this paper could also be used for assay of methemoglobin in a whole blood sample caused by poisoning by CO, NO, etc. Immunomagnetic cell sorting by tagging specific cell surface epitopes with magnetic particle conjugates has been gaining popularity in the fields of cell biology and medical

microbiology [35–37]. Besides blood cell sorting based on their native magnetic properties, a microfluidic chip like the one proposed in this work could also be used as a general platform for continuous cell sorting with magnetic labeling for diagnostic purposes [38–40]. An application study is in progress in our laboratory.

Acknowledgements Financial support from Northeastern University is acknowledged. The authors are grateful to Hong-Zhuan Yin from the Chinese Medicine University for fruitful discussions.

References

1. Takayasu M, Kelland DR, Minervini JV, Friedlaender FJ, Ash SR (1999) Paper presented at IWCPB-HMF (international workshop on chemical, physical and biological processes under high magnetic fields), Omiya, Saitame, Japan, 24–26 November
2. Han KH, Frazier AB (2006) *Lab Chip* 6:265–273
3. Melville D, Paul F, Roath S (1975) *Nature* 255:706
4. Owen CS (1978) *Biophys J* 22:171–178
5. Takayasu M, Duske N, Ash SR, Friedlaender FJ (1982) *IEEE Trans Magn Mag* 18(6):1520
6. Takayasu M, Kelland DR, Minevini JV (1999) Paper presented at 16th international conference on magnet technology, Florida, USA, 26 September–2 October
7. Zborowski M, Osters GR, Moore LR, Milliron S, Chalmers JJ, Schechter AN (2003) *Biophys J* 84:2638–2645
8. Han KH, Frazier AB (2005) *NSTI-Nanotech* 1:187–190
9. Han KH, Frazier AB (2004) *J Appl Phys* 96:5797–5802
10. Yi CQ, Li CW, Ji SL, Yang MS (2006) *Anal Chim Acta* 560:1–23
11. Li XJ, Li PCH (2005) *Anal Chem* 77:4315–4322
12. Yang MS, Li CW, Yang J (2002) *Anal Chem* 74:3991–4001
13. Furdui VI, Harrison DJ (2004) *Lab Chip* 4:614–618
14. Grodzinski P, Yang J, Liu RH, Ward MD (2003) *Biomed Microdevices* 5:303–310
15. Inglis DW, Riehn R, Austin RH, Sturm JC (2004) *Appl Phys Lett* 85:5093–5095
16. Enger J, Goksor M, Ramser K, Hagberg P, Hanstorp D (2004) *Lab Chip* 4:196–200
17. Chiou PY, Ohta AT, Wu MC (2005) *Nature* 436:370–372
18. Brody JP, Osborn TD, Forster FK, Yager P (1996) *Sens Actuators A* 54:704–708
19. Crowley TA, Pizziconi V (2005) *Lab Chip* 5:922–929
20. Chen X, Cui DF, Liu CC, Li H (2007) *Sens Actuators B*. doi:10.1016/j.snb.2007.07.126
21. Chou C, Morgan M, Zenhausem F, Prinz C, Austin R (2002) *MicroTAS* 25–27
22. Durr M, Kentsch J, Muller T, Schnelle T, Stelzle M (2003) *Electrophoresis* 24:722–731
23. Huang Y, Joo S, Duhon M, Heller M, Wallace B, Xu X (2002) *Anal Chem* 74:3362–3371
24. Gill R, Freeman R, Xu JP, Willner I, Wingograd S, Shweky I, Banin U (2006) *J Am Chem Soc* 128:15376–15377
25. Wu SM, Zhao X, Zhang ZL, Xie HY, Tian ZQ (2006) *Chemphyschem* 7:1062–1067
26. Jiang C, Xu SK, Yang DZ, Zhang FH, Wang WX (2007) *Luminescence* 22:430–437
27. Xie M, Liu HH, Chen P, Zhang ZL, Wang XH, Xie ZX, Du YM, Pan BQ, Pang DW (2005) *Chem Commun* 44:5518–5520
28. Jaiswal JK, Simon SM (2004) *Trends Cell Biol* 14:497–504
29. Fang F, Wu ZY (2006) *Chin Patent Appl* 200610047737.4

30. Yin XF, Shen H, Fang ZL (2003) *Chin J Anal Chem* 31:116–119
31. Fang DF, Zhou L, Ding L, Zhang DC (1995) *Modern medicinal research technology manual*. Union Press of Peking University of Medical Science and Peking Union Medical College, Beijing
32. Chen QF, Wang WX, Ge YX, Xu SK, Yang DZ (2007) *Chin J Anal Lab* 26:1–5
33. Moeser GD, Roach KA, Green WH, Hatton TA, Laibinis PE (2004) *AIChE J* 50:2835–2848
34. Qiu JC (1987) *Mineral processing technology*. Metallurgical Industry, Beijing
35. Charles N, Liesveld JL, King MR (2007) *Biotechnol Prog* 23:1463–1472
36. McCloskey KE, Chalmers JJ, Zborowski M (2003) *Anal Chem* 75:6868–6874
37. Kuhara M, Takeyama H, Tanaka T, Matsunaga T (2004) *Anal Chem* 76:6207–6213
38. Xie HY, Zuo C, Liu Y, Zhang ZL, Pang DW, Li XL, Gong JP (2005) *Small* 5:506–509
39. Wang GP, Song EQ, Xie HY, Zhang ZL, Tian ZQ, Zuo C, Pang DW, Wu DC, Shi YB (2005) *Chem Commun* 34:4276–4278
40. Liu YJ, Guo SS, Zhang ZL, Huang WH, Baigl D, Xie M, Chen Y, Pang DW (2007) *Electrophoresis* 28:4713–4722